

## HUMAN MOTION ANALYSIS AND MEASUREMENT TECHNIQUES: CURRENT APPLICATION AND DEVELOPING TREND

*Yang Song*<sup>1,2</sup>, *József Sárosi*<sup>2</sup>, *Xuanzhen Cen*<sup>1,2</sup>, *István Bíró*<sup>2</sup>

1. Doctoral School on Safety and Security Sciences, Óbuda University, Bécsi str 96. 1034, Budapest, Hungary

2. Faculty of Engineering, University of Szeged, Mars tér 7. 6724, Szeged, Hungary

Corresponding authors, Yang Song; e-mail: yang.song@uni-obuda.hu

### ABSTRACT

Human motion analysis and measurement technology have been widely used in the fields of medical treatment, sports science, and rehabilitation. In clinical practice, motion analysis has been applied in the diagnosis and individualized treatment planning of various musculoskeletal diseases, and it is also an important objective scientific method to evaluate the therapeutic effect and the effectiveness of medical equipment. This study aimed to introduce the common modern motion capture measurement technology and equipment, the clinical application and limitations of motion analysis, and the possible development trend of motion analysis measuring techniques in the future. Motion analysis and measurement systems and medical image measurement and analysis technology have made landmark improvements over the past few decades in terms of orthopaedic biomechanics. Nevertheless, limitations still exist, both subjective and objective. All these drawbacks have promoted the exploration of the integrated methods that have now been widely used in motion analysis. The results of the case study about the subject-specific finite element modeling of the foot and sports shoe complex have also shown great consistency. Nevertheless, several possible future directions for motion analysis measuring techniques still exist. In the future, the progress of motion analysis and measurement methods will simultaneously drive the progress of orthopedics, rehabilitation, precision personalized medicine, and medical engineering.

Keywords: sports biomechanics, motion analysis, measuring techniques

### 1. INTRODUCTION

Motion analysis, as the name implies, is a science of studying human movement. Early studies of human motion analysis aimed to understand the movement of the human body during various activities and to analyze the movement into many minute moments [1]. Through the analysis and study of the movement process, it can simplify the movement process, facilitate the standardization of movement, and improve the efficiency of movement. With the development and progress of science and technology, modern motion analysis is based on scientific means to measure the motion characteristics of the human body and the mechanical performance of each joint, quantitative analysis of the relative motion of each limb, the force borne by the joint [2], [3]. At present, motion analysis and measurement technology has been widely used in many fields such as medical treatment [4], sports science [2], and rehabilitation [5], and plays an indispensable role in improving the accuracy of surgery, implementing rehabilitation actions, and monitoring the process of daily activities.

In clinical practice, motion analysis has been applied in the diagnosis and individualized treatment planning of various musculoskeletal diseases [6], and it is also an important objective scientific method to evaluate the therapeutic effect and the effectiveness of medical equipment [7]. In the future, the progress of motion analysis and measurement methods will simultaneously drive the progress of orthopedics, rehabilitation, precision personalized medicine, and medical engineering. The main purposes of this study were to introduce the common modern motion capture measurement technology and equipment, the clinical application and limitations of motion analysis, and the possible development direction of motion analysis measuring techniques in the future. In addition, a case study in terms of the subject-specific finite element modeling of the foot and sports shoe complex was further performed for further elaborate explanation of the integrated method that is widely used in human motion capture and analysis.

## 2. MOTION CAPTURE MEASUREMENT AND ANALYSIS TECHNOLOGY AND EQUIPMENT

Modern motion analysis and measurement system, mainly through the application of different technologies to track the movement trajectory of the reflective marker ball pasted on the skin, with multi-link motion model, calculate joint motion (Figure 1) [3]. Based on the motion parameters, the mass parameters of different limbs, and the ground reaction force measured by the force plate, the resultant force and torque of each joint are obtained by inverse dynamic analysis and calculation based on Newton's laws of mechanics [3]. The main common motion capture equipment can be divided into optical, electromagnetic, and inertial measurement devices.

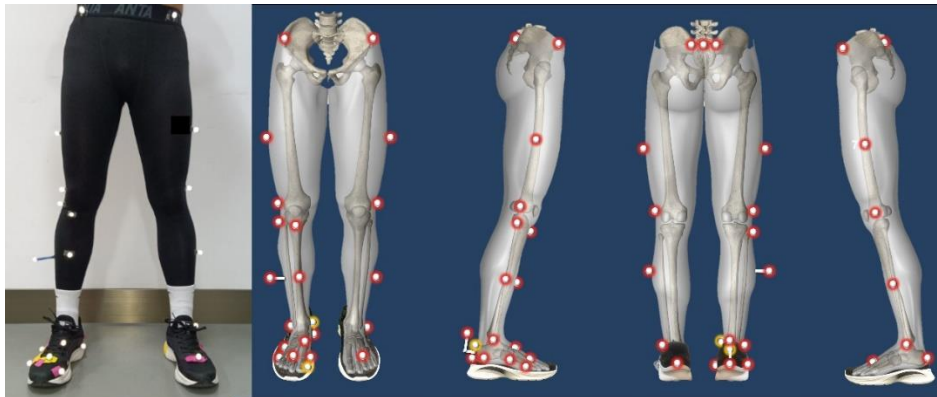


*Figure 1. The reflective marker ball pasted on the skin*

### 2.1. Optical motion capture measuring techniques

The motion capture system using infrared reflective markers and infrared cameras is the most common and widely used optical motion analysis and measurement equipment [8]. Multiple infrared cameras are used to record the position of the reflector on the image, and with image processing, the position of the reflector center on the image can be automatically calculated [9]. Direct linear transformation and stereophotogrammetry can be used to calculate the three-dimensional trajectory of the center point of the reflector in space if the same reflector can be captured by more than two cameras at the same time [10]. By using this system, the coordinate system of an object can be defined with only three reflective marks pasted on the object, and then the position and direction of the object in space can be accurately described [9]. However, the traditional motion analysis and measurement system using multiple cameras and system host is bulky, inconvenient to move, and expensive, which is greatly limited in application and has obstacles in the clinical promotion. In recent years, some researchers have developed a small, portable, and convenient 3D joint dynamic measurement system using digital navigation equipment [11]. Due to the fixed relative position of the two cameras, the system does not need to be corrected before use. Through the modular design and the tracking of the infrared reflective ball, the small 3D dynamic joint measurement system can dynamically digitize the kinematic characteristics of the living joint in the bearing state and the functional motion process, which is of great value to promote the motion analysis for real-time diagnosis and field application in clinical hospitals. However, infrared equipment may be limited to signal interference caused by excessive strong infrared in outdoor sunny places, which will cause difficulties and errors in measurement [12].

## 2.2. Electromagnetic motion capture measuring techniques

Electromagnetic motion tracking measurement equipment, the use of electromagnetic emission equipment in space to generate a magnetic field, through several sensors attached to different limb segments, sensing the movement of the magnetic field changes, to calculate the sensor in space position and direction [13]. The device can measure six degrees of freedom using a single sensor, but due to the weight and volume of the sensor, it can affect the movement when used. When using an electromagnetic tracking device, it is important to pay attention to electromagnetic field changes caused by the surrounding environment, which may affect the measurement accuracy. For example, metal components around the measurement site may interfere with electromagnetic fields [13].

## 2.3. Inertial motion capture measuring techniques

Inertial motion analysis and measurement devices mainly use gyroscopes and accelerometers [14]. Due to the development of modern micromotors, accelerometers and gyroscopes can be miniaturized, easy to carry, and have been widely used in smart devices such as mobile phones [15]. Due to its low power consumption and no need for external capture equipment, it can be used to track human movement for a long time. In addition, the diagonal acceleration and linear acceleration can be integrated twice to find the position and angle of the object in space. However, there will be errors in the integration process, and serious errors may accumulate over a long period [14].

## 2.4. Summary

The motion analysis method of measurement is in the human body surface paste tag or sensing component, to mark or inductive component changes to represent human movement. However, the skin and bone are separated by soft tissue, which will cause soft tissue deformation when the human body moves, resulting in relative displacement between the sensor component and the underlying bone, which is one of the biggest sources of error in motion analysis technology: soft tissue movement error. The invasive method uses bone nails to attach reflective markers or sensors to the bone directly. Although the method directly and accurately measures bone movement, invasive techniques limit the natural movement of soft tissue over the bone, impair movement and expose subjects to the risk of infection. Due to ethical issues, the application of invasive methods in motion measurement in vivo has been greatly limited, but there are still some studies on animal models. Therefore, the development of a non-invasive and accurate motion analysis measurement method is an inevitable means to measure the motion parameters of the joint in the natural functional motion of the living body.

## 3. MEDICAL IMAGE MEASUREMENT AND ANALYSIS TECHNOLOGY AND EQUIPMENT

### 3.1. X-ray related image measurement and analysis technology

The discovery of X-rays and the development of medical imaging technology have provided the opportunity to measure bone directly in a non-invasive way. With traditional X-ray, bone images can be taken directly for two-dimensional measurement and analysis. However, due to the source of two-dimensional images, although the rotation angle in other directions can be calculated mathematically, the error of the estimated value is large [16].

X-ray stereography, in which small tantalum sphere markers are embedded in the object, uses two X-ray imaging systems to simultaneously image the small tantalum sphere object and further mathematically obtain the three-dimensional spatial position of the object. The position can be measured with an accuracy of 10-250  $\mu\text{m}$  and the angle can be 0.03-0.6°, making it a highly accurate method of 3D kinematic measurement [17]. At present, X-ray stereography is used in a wide range of fields, such as oncology, odontology, and

clinical procedures such as plastic surgery and neurosurgery [18]. Although accurate, this method is invasive and can only be used for static position measurements [18]. Dynamic X-ray systems (Fluoroscopy), which take continuous dynamic images [19]. Most current dynamic X-ray systems are image intensifier imaging systems that convert invisible X-rays into visible light for imaging, but the imaging process is influenced by the shape of the input fluoroscope and the X-ray electron beam is influenced by the surrounding electromagnetic field [19]. The geometry of the output phosphor screen itself and the characteristics of the subsequent video equipment can also cause image distortion, so the output image needs to be image corrected before it can be analyzed. However, the image data obtained with dynamic X-ray technology is also limited to two dimensions and does not provide a complete picture of the three-dimensional movement of the body's joints [20].

The use of uniplanar dynamic X-rays without implantation of markers for 3D motion measurement was introduced by Scott Banks [21]. He uses the clear visibility of the artificial total knee joint on X-ray to record continuous images of the motion of the joint on dynamic X-ray and then compares the contours of the X-ray image with the contours of the model projection using a computerized three-dimensional model of the artificial total knee joint. The comparison algorithm uses the Fourier descriptor proposed by Wallace et al. [22] to describe each contour, and the differences in the Fourier descriptors between the contours are used to find the optimal spatial position of the artificial total knee joint. Once the positions of the artificial joint components are obtained, the motion of the artificial total knee joint is further calculated. However, the point-source projection model of the single-plane dynamic X-ray system has an inherent flaw in that the magnification of the image decreases when the measured object is moved away from the X-ray source, resulting in large errors in out-of-plane translation and inability to accurately measure the motion of the joint in six degrees of freedom [23].

Since then, Li et al. [24] and Tashman et al. [25] have developed a dual-plane dynamic X-ray tracking measurement technique, respectively. The method uses two 2D dynamic X-ray images and a 3D skeleton model and uses optimization to compare the 3D model and the 2D image in both planes to find the best matching 3D model position to find the 3D motion during functional movements of a living joint. This technique has been applied to all major joints in the human body, including the hip, knee, spine, and ankle [26]. However, due to the size of the imaging plane and the radiation dose of the X-rays, the dual-plane dynamic X-ray method can only be used for localized joint motion measurements and is unable to observe whole body joint motion at the same time.

### **3.2. CT and MRI related image measurement and analysis technology**

Computer tomography (CT) and magnetic resonance imaging (MRI) methods can produce a range of skeletal and soft tissue cross-sectional images that can be analyzed and stacked to obtain accurate three-dimensional reconstructions of skeletal models and the relative position of joint bones [27], [28]. However, this method cannot be used to measure dynamic movements, to quantify in vivo joint movements and, due to the location of the CT and MRI machines, it is often not possible to measure the human body in a weighted position.

## **4. INTEGRATED MEASUREMENT AND ANALYSIS TECHNOLOGY AND EQUIPMENT**

Clearly, motion analysis and measurement systems and medical image measurement and analysis technology have made landmark improvements over the past few decades in terms of orthopaedical biomechanics. Nevertheless, limitations still exist, both subjective and objective. All these drawbacks have promoted the exploration and development of other integrated solutions. This section aims to introduce one of the current integrated methods that have been widely used in motion analysis.

## 4.1. General workflow of the integrated method for orthopaedical biomechanics

Figure 2 illustrates the basic experimental workflow of the above integrated method for orthopaedical biomechanics using the Vicon motion capture system, OpenSim, and ANSYS. First, the kinematic and kinetic data during motion were collected using 3D marker-based optoelectronic system and then convert into OpenSim based on MATLAB or other software. Second, the following several steps were applied to build a musculoskeletal model based on the above data. The initial step “Scaling” was performed to adjust the anthropometric differences and obtain the personalization matched model. Then the “Inverse Kinematics” and “Inverse Dynamics” were conducted to further load the experimental motion and force. The “Static Optimization” and “Computed Muscle Control” were employed to calculate the muscle activation and muscle forces induced during the experimental motion. Finally, the personalized musculoskeletal model could be used for kinematic, kinetic, and electromyography comparison. On the other hand, the medical CT images were collected by scanning the participant’s soft tissue. The DICOM images then were segmented by MIMIC to obtain the boundaries of bones, soft tissues, and build the 3D geometry model. These geometries were smoothed using Geomagic Wrap and then imported into Solidworks to form solid parts. Finally, the built model was imported to ANSYS for investigating the internal reaction between joints. For example, Yu et al. (2021) [29] investigated knee joints during badminton directional lunges by using the above workflow. The biomechanical data from the motion capture system were used for musculoskeletal modeling under OpenSim, and the calculated joint kinematics and muscle forces were used as boundary conditions for finite element analysis of the knee joint.

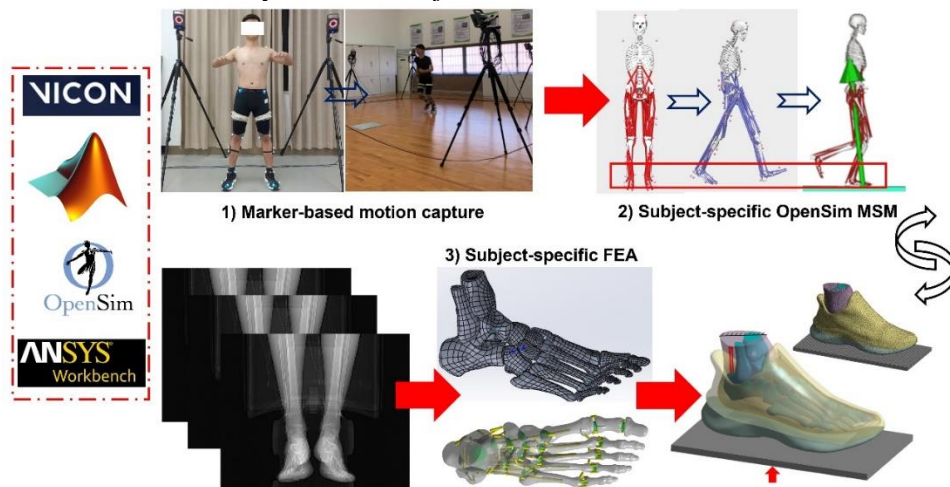


Figure 2. Basic experimental workflow of the current integrated method for motion analysis (Foot simulation for example)

## 4.2. Case study using the integrated method for orthopaedical biomechanics

In order to further elaborate the integrated method for orthopaedical biomechanics, a case study about the subject-specific finite element modelling of the foot and sports shoe complex was performed.

### 4.2.1 Coupled foot-shoe modelling

In this study, a computer tomography (CT) device (Optima CT540, GE Healthcare, Chicago, USA) was used to perform cross-sectional scans on the right foot of the subjects wearing sports shoes to obtain medical image data of the foot shoes. The corrective brace placed the subject's ankle in a neutral position. The obtained foot-shoe DICOM format image data was imported into MIMIC 21.0 software (Materialise, Leuven,

Belgium) for 3D geometric inverse modelling of foot bones, soft tissues, and sports shoes. Among them, based on ensuring the overall outline of the sneaker and the thickness of each part, the noise pixels between the foot and the shoe are further manually deleted to realize the non-complete contact between the foot and the shoe and establish a sports shoe model with internal cavities. In addition, in order to improve the efficiency of simulation calculation, this study simplifies some models, mainly including fusion of the second to fifth distal phalanges with their corresponding proximal phalanges; sports socks and soft tissue fusion; sports shoes are divided into upper and sole two parts. The surface model obtained by the above inverse modelling was smoothed by Geomagic Wrap 2017 software (3D Systems, South Carolina, USA) and imported into Solidworks 2020 software (Dassault Systèmes, France) for further solidification.

In order to realize the interconnection and relative motion between the bones of the foot, this study further modeled the main cartilages, ligaments, and plantar fascia of the foot according to the anatomy of the ankle. As shown in Figure 3, the finite element model of the foot consists of 20 bones, 1 soft tissue, 20 cartilage, 66 ligaments, and 5 plantar fascia. Subsequently, the overall foot-shoe solid model was imported into the Mechanical Model module of the ANSYS Workbench 2021 software (ANSYS, Inc., Canonsburg, USA) for meshing. The ligaments and plantar fascia were modelled with two-node wire-body elements. Except for the support plate which uses hexahedral elements, the rest of the solid models are meshed with tetrahedral elements. Among them, the soft tissue, sports shoes, and support plate mesh elements are 5mm, the bone is 3.5mm, and the cartilage is 2mm. The final model has a total of 358,322 nodes and 208,225 mesh elements.



**Figure 3.** The coupled foot-shoe finite element model

All the tissue modules of the foot-shoe model in this study are set as a single isotropic linear elastic material, and its material properties are defined by Young's modulus and Poisson's ratio. Among them, the material mechanical parameters of the foot bone are defined according to the volume ratio of cortical bone and cancellous bone, and the material parameters of cartilage, ligament, soft tissue, sports shoes, and support plate are also taken from previous relevant finite element studies. In addition, in order to further explore the biomechanical effects of different sole materials on the foot, Young's modulus parameters were treated as  $\pm 10\%$  and  $\pm 20\%$  on the existing basis, namely 2.490MPa (0%), 2.739MPa (+10%), 2.241MPa (-10%), 2.988MPa (+20%), 1.992MPa (-20%).

Since the change of plantar pressure during the simulation process has a certain correlation with the relative angle of the foot in the 3D plane, this study adopts the Vicon 3D motion capture system (Vicon Metrics Ltd., Oxford, UK) to record the position parameters of the reflective mark points of the feet when the subjects are standing statically, and further calculate the spatial sagittal and coronal planes of the feet through the projection vector of the foot rigid body coordinate system (XYZ) on the spatial coordinate system. The center point of the lower edge of the heel bone is defined as the origin of the rigid body coordinate system, the X-axis points to the middle point of the line connecting the first metatarsal and the fifth phalanx, the Z-axis is perpendicular to the X-axis and is vertically upward, and the Y-axis is perpendicular to the plane where the

XZ axis is located. The AMTI 3D force plate (AMTI, Watertown, Massachusetts, USA) is synchronized with the Vicon motion capture system to collect the vertical ground reaction force (343.00N) when the subject is statically standing. It is applied to the center of the bottom surface of the support plate, and the direction is vertical upward. Previous studies have shown that when the human body is standing with static balance on both feet, the force of the lower triceps calf is about half of the foot load. Therefore, in this paper, a force of 171.50N is applied vertically upward at the calcaneal node in the form of a concentrated load to simulate the triceps force.

The boundary conditions of the model are set as shown in Figure 4, in which the upper surfaces of the soft tissue, tibia, and fibula are set to be completely fixed. The support plate is set to only move up and down, and other directions are completely constrained. The frictional contact between the soft tissue surface and the shoe cavity and between the sole and the upper surface of the support plate is defined as a friction coefficient of 0.6.

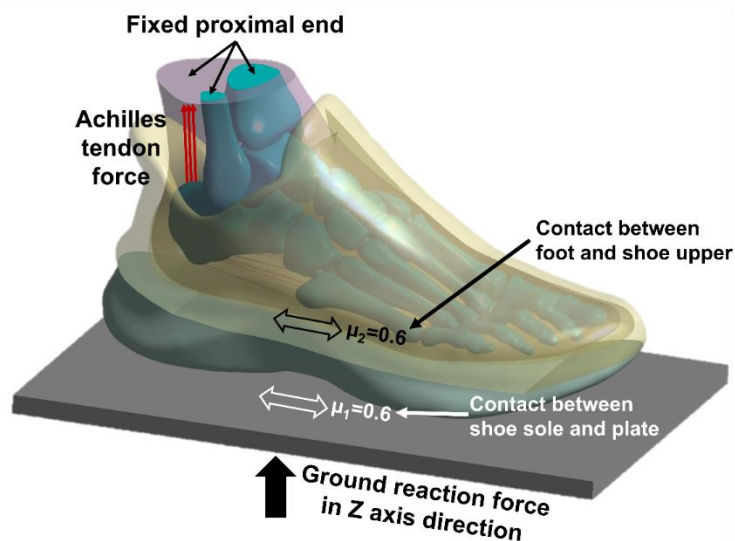


Figure 4. Boundary and loading condition

In this study, the pressure distribution of the foot sole and shoe outsole during static standing was synchronously collected by the Pedar insole pressure sensing system and the emed pressure plate (Novel GmbH, Munich, Germany), and was compared with the pressure cloud map obtained by the finite element simulation to verify the above-mentioned foot-sport shoe finite element model.

#### 4.2.2 Model verification and simulation results

By comparing the pressure cloud diagrams of the finite element simulation and the experimental test, it is found that the pressure distributions of the foot sole and shoe outsole measured by the two methods are basically the same. Among them, the foot sole pressure is concentrated in the heel area, followed by the medial forefoot, the lateral forefoot, and the midfoot area. The shoe outsole pressure is concentrated in the medial area, namely the anteromedial area and the posteromedial area, followed by the anterolateral area and the posterolateral area.

Figure 5 shows the cloud map of the metatarsal stress distribution under the condition of barefoot and shoes with different outsole material parameters. It can be seen from the observation that the stress concentration is distributed at the bottom of the second and third metatarsal bodies under the static standing condition, and the third metatarsal is subjected to the greatest stress. Compared with the barefoot state, the peak stress in

the metatarsal region decreased significantly (2.876MPa) when standing with shoes on. However, with the increase of the stiffness of the sole material, the peak stress in the metatarsal region also gradually increased, but both were smaller than the peak stress in the barefoot state (5.096MPa).

In addition, through further analysis of the peak stress of each metatarsal (Figure 6), it was found that compared with the barefoot, the difference in the peak stress of each metatarsal was smaller when standing with shoes on. However, with the increase of the stiffness of the sole material, the first and fourth the stress peak value of the fifth metatarsal gradually decreased, the peak stress value of the second and third metatarsal bones gradually increased, and the peak stress difference between the metatarsal bones increased, and the stress tended to be concentrated, but it was still smaller than the peak stress difference between the metatarsal bones in barefoot.

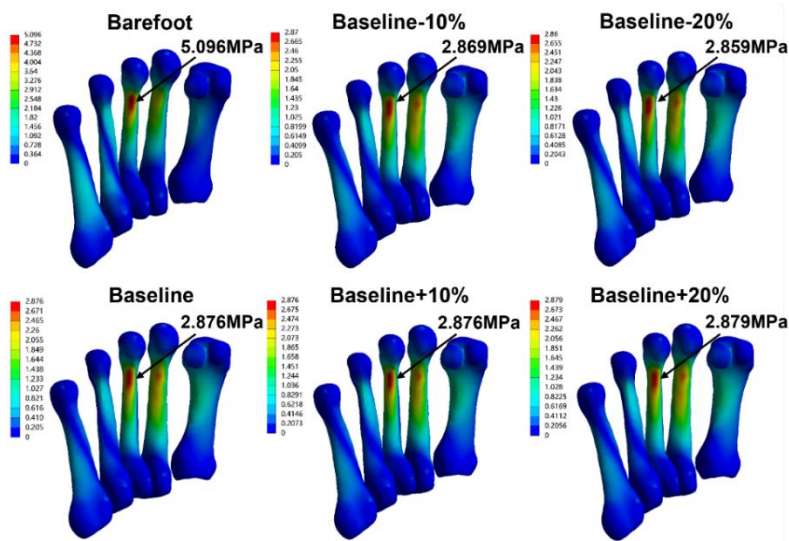


Figure 5. Predicted peak metatarsal von Mises stress and its distribution under barefoot or shod situations

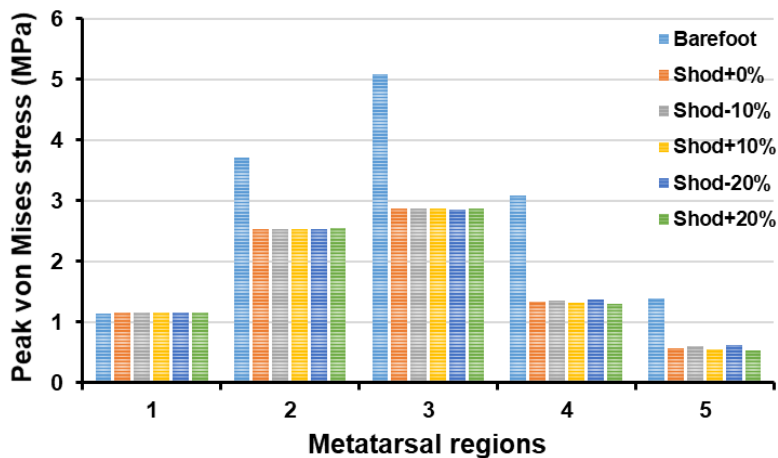


Figure 6. Predicted peak von Mises stress of each metatarsal under barefoot or shod situations

## 4. LIMITATION AND FUTURE DIRECTIONS

Although motion analysis has been applied to many clinical issues and can provide a lot of information for interpretation and assessment by clinical staff, such as for real-time tracking of surgery, surgical navigation, measurement of the subject's usual activity level, sleep quality, guidance on rehabilitation movements, monitoring of falls in the elderly [30], [31], [32], etc., motion analysis still has its shortcomings. The main issues are the high cost of motion analysis equipment, the time taken to affix markers, and the inadequate design of the analysis software. Clinical staff are often limited by hardware and software technology and are unable to apply it to many different patients. The estimation of intra-articular forces during human movement remains one of the greatest challenges in biomechanical research, and current motion analysis techniques still do not provide information on intra-articular forces in a non-invasive way. Current research using non-invasive methods is still limited to exploring kinematic and kinetic related variables in live motion, including joint angles, displacements, and moments.

The use of motion analysis for the assessment and diagnosis of neuromuscular disorders has merit and necessity, and scientifically quantified motion analysis tools will continue to play an important role in the fields of clinical orthopedics and rehabilitation engineering. For example, motion analysis techniques can be used to capture the manifestation of joint instability in all directions to aid in the diagnosis of sports injuries and to assess the performance of patients after they have received different treatments, aids, and implants, which can be fed back into therapy to correct abnormal joint movements or parameters and assist patients in regaining normal function [2], [33], [34].

There are several possible future directions for motion analysis measuring techniques. Firstly, to reduce the impact of skin movement errors and improve the accuracy of current methods of motion analysis; secondly, to develop marker-less analysis systems to make the application of motion analysis easier and save preparation time; thirdly, to develop mechanical and kinematic sensor technology that can be routinely placed inside artificial implants to record internal skeletal forces and motion data; and finally, the development of easier to use, more affordable and portable motion analysis systems will facilitate the development of more applications for clinical motion analysis.

## REFERENCES

- [1] J. K. Aggarwal, Q. Cai, Human Motion Analysis: A Review, *Computer vision and image understanding*, Vol. 73, 1999, pp. 428–440  
<https://doi.org/10.1006/cviu.1998.0744>
- [2] D. Sun, G. Fekete, J. S. Baker, Y. Gu, Foot motion character during forward and backward walking with shoes and barefoot, *Journal of Motor Behavior*, Vol. 52, 2020, pp. 214–225  
<https://doi.org/10.1080/00222895.2019.1605972>
- [3] F. Patrona, A. Chatzitofis, D. Zarpalas, P. Daras, Motion analysis: Action detection, recognition and evaluation based on motion capture data, *Pattern Recognition*, Vol. 76, 2018, pp. 612–622  
<https://doi.org/10.1016/j.patcog.2017.12.007>
- [4] G. A. Bello, T. J. W. Dawes, J. Duan, C. Biffi, A. de Marvao, L. S. G. E. Howard, J. S. R. Gibbs, M. R. Wilkins, S. A. Cook, D. Rueckert, D. P. O'Regan, Deep-learning cardiac motion analysis for human survival prediction, *Nature machine intelligence*, Vol. 1, 2019, pp. 95–104  
<https://doi.org/10.1038/s42256-019-0019-2>
- [5] W. J. Sohn, R. Sipahi, T. D. Sanger, D. Sternad, Portable Motion-Analysis Device for Upper-Limb Research, Assessment, and Rehabilitation in Non-Laboratory Settings, *IEEE Journal of Translational Engineering in Health and Medicine*, Vol. 7, 2019, pp. 1–14  
<https://doi.org/10.1109/JTEHM.2019.2953257>
- [6] D. Shim, J. Y. Choi, S. Yi, E. S. Park, S. Kim, B. Yoo, D. Park, H. Park, D. Rha, Spatiotemporal parameters from instrumented motion analysis represent clinical measurement of upper limb function in children with cerebral palsy, *Gait & Posture*, Vol. 91, 2022, pp. 326–331

- <https://doi.org/10.1016/j.gaitpost.2020.11.007>
- [7] M. T. Parks, Z. Wang, K. C. Siu, Current Low-Cost Video-Based Motion Analysis Options for Clinical Rehabilitation: A Systematic Review, *Physical therapy*, Vol. 99, 2019, pp. 1405–1425  
<https://doi.org/10.1093/ptj/pzz097>
- [8] E. van der Kruk, M. M. Reijne, Accuracy of human motion capture systems for sport applications; state-of-the-art review, *European journal of sport science*, Vol. 18, 2018, pp. 806–819  
<https://doi.org/10.1080/17461391.2018.1463397>
- [9] D. C. Wierschem, J. A. Jimenez, F. A. Méndez Mediavilla, A motion capture system for the study of human manufacturing repetitive motions, *The International Journal of Advanced Manufacturing Technology*, Vol. 110, 2020, pp. 813–827  
<https://doi.org/10.1007/s00170-020-05822-9>
- [10] H. Hatze, High-precision three-dimensional photogrammetric calibration and object space reconstruction using a modified DLT-approach, *Journal of biomechanics*, Vol. 21, 1988, pp. 533–538  
[https://doi.org/10.1016/0021-9290\(88\)90216-3](https://doi.org/10.1016/0021-9290(88)90216-3)
- [11] Y. Zhang, Z. Yao, S. Wang, W. Huang, L. Ma, H. Huang, H. Xia, Motion analysis of Chinese normal knees during gait based on a novel portable system, *Gait & Posture*, Vol. 41, 2015, pp. 763–768  
<https://doi.org/10.1016/j.gaitpost.2015.01.020>
- [12] Mr. Naeemabadi, B. Dinesen, O. K. Andersen, J. Hansen, Investigating the impact of a motion capture system on Microsoft Kinect v2 recordings: A caution for using the technologies together, *PLoS One*, Vol. 13, 2018, pp. e0204052  
<https://doi.org/10.1371/journal.pone.0204052>
- [13] K. N. An, M. C. Jacobsen, L. J. Berglund, E. Y. S. Chao, Application of a magnetic tracking device to kinesiological studies, *Journal of biomechanics*, Vol. 21, 1988, pp. 613–620  
[https://doi.org/10.1016/0021-9290\(88\)90225-4](https://doi.org/10.1016/0021-9290(88)90225-4)
- [14] C. Verplaetse, Inertial proprioceptive devices: Self-motion-sensing toys and tools, *IBM Systems Journal*, Vol. 35, 1996, pp. 639–650  
<https://doi.org/10.1147/sj.353.0639>
- [15] Z. H. Kareem, K. N. bin Ramli, R. Q. Malik, M. M. A. Zahra, Mobile phone user behavior's recognition using gyroscope sensor and ML algorithms, *Materials Today: Proceedings*, 2021  
<https://doi.org/10.1016/j.matpr.2021.04.639>
- [16] P. A. Torzilli, R. L. Greenberg, J. Insall, An in vivo biomechanical evaluation of anterior-posterior motion of the knee. Roentgenographic measurement technique, stress machine, and stable population, *JBJS*, Vol. 63, 1981, pp. 960–968
- [17] G. Selvik, Roentgen stereophotogrammetry: A method for the study of the kinematics of the skeletal system, *Acta Orthopaedica Scandinavica*, Vol. 60, 1989, pp. 1–51  
<https://doi.org/10.3109/17453678909154184>
- [18] R. A. Sherlock, W. M. Aitken, A method of precision position determination using X-ray stereography, *Physics in Medicine & Biology*, Vol. 25, 1980, pp. 349–355  
<https://doi.org/10.1088/0031-9155/25/2/016>
- [19] M. A. Pritchett, S. Schampaert, J. A. H. de Groot, C. C. Schirmer, I. van der Bom, Cone-Beam CT With Augmented Fluoroscopy Combined With Electromagnetic Navigation Bronchoscopy for Biopsy of Pulmonary Nodules, *Journal of bronchology & interventional pulmonology*, Vol. 25, 2018, pp. 274–282  
<https://doi.org/10.1097/LBR.0000000000000536>
- [20] D. L. Miller, Overview of contemporary interventional fluoroscopy procedures, *Health physics*, Vol. 95, 2008, pp. 638–644  
<https://doi.org/10.1097/01.HP.0000326341.86359.0b>
- [21] S. A. Banks, Model based 3D kinematic estimation from 2D perspective silhouettes: application with total knee prostheses, *Massachusetts Institute of Technology*, 1992
-

- [22] T. P. Wallace, P. A. Wintz, An efficient three-dimensional aircraft recognition algorithm using normalized fourier descriptors, *Computer Graphics and Image Processing*, Vol. 13, 1980, pp. 99–126  
[https://doi.org/10.1016/S0146-664X\(80\)80035-9](https://doi.org/10.1016/S0146-664X(80)80035-9)
- [23] Laurentini, How far 3D shapes can be understood from 2D silhouettes, *IEEE Transactions on Pattern Analysis and Machine Intelligence*, Vol. 17, 1995, pp. 188–195  
<https://doi.org/10.1109/34.368170>
- [24] G. Li, T. H. Wuerz, L. E. DeFrate, Feasibility of Using Orthogonal Fluoroscopic Images to Measure In Vivo Joint Kinematics, *Journal of Biomechanical Engineering*, Vo. 126, 2004, pp. 313–318  
<https://doi.org/10.1115/1.1691448>
- [25] S. Tashman, W. Anderst, In-Vivo Measurement of Dynamic Joint Motion Using High Speed Biplane Radiography and CT: Application to Canine ACL Deficiency, *Journal of Biomechanical Engineering*, Vol. 125, 2003, pp. 238–245  
<https://doi.org/10.1115/1.1559896>
- [26] R. J. de Asla, L. Wan, H. E. Rubash, G. Li, Six DOF in vivo kinematics of the ankle joint complex: Application of a combined dual-orthogonal fluoroscopic and magnetic resonance imaging technique, *Journal of Orthopaedic Research*, Vol. 24, 2006, pp. 1019–1027  
<https://doi.org/10.1002/jor.20142>
- [27] Y. Zhang, J. Awrejcewicz, J. S. Baker, Y. Gu, Cartilage stiffness effect on foot biomechanics of Chinese bound foot: A finite element analysis, *Frontiers in Physiology*, Vol. 9, 2018, pp. 1434  
<https://doi.org/10.3389/fphys.2018.01434>
- [28] Q. Zhang, T. Chon, Y. Zhang, J. S. Baker, Y. Gu, Finite element analysis of the lumbar spine in adolescent idiopathic scoliosis subjected to different loads, *Computers in Biology and Medicine*, Vol. 136, 2021, pp. 104745  
<https://doi.org/10.1016/j.compbiomed.2021.104745>
- [29] L. Yu, Q. Mei, N. I. Mohamad, Y. Gu, J. Fernandez, An exploratory investigation of patellofemoral joint loadings during directional lunges in badminton, *Computers in Biology and Medicine*, Vol. 132, 2021, pp. 104302  
<https://doi.org/10.1016/j.compbiomed.2021.104302>
- [30] Y. Song, F. Ren, D. Sun, M. Wang, J. S. Baker, B. István, Y. Gu, Benefits of exercise on influenza or pneumonia in older adults: a systematic review, *International Journal of Environmental Research and Public Health*, Vol. 17, 2020, pp. 2655  
<https://doi.org/10.3390/ijerph17082655>
- [31] A. Sim, S. Mukherjee, Potential Low Energy Availability (LEA) risk amongst amateur and recreational athletes in Singapore, *Physical Activity and Health*, Vol. 5, 2021, pp. 166-177  
<http://doi.org/10.5334/paah.120>
- [32] Y. He, G. Fekete, The Effect of Cryotherapy on Balance Recovery at Different Moments after Lower Extremity Muscle Fatigue, *Physical Activity and Health*, Vol. 5, 2021, pp. 255-270  
<http://doi.org/10.5334/paah.154>
- [33] D. Sun, G. Fekete, J. S. Baker, Q. Mei, B. István, Y. Zhang, Y. Gu, A Pilot Study of Musculoskeletal Abnormalities in Patients in Recovery from a Unilateral Rupture-Repaired Achilles Tendon, *International Journal of Environmental Research and Public Health*, Vol. 17, 2020, pp. 4642  
<https://doi.org/10.3390/ijerph17134642>
- [34] X. Jiang, H. Chen, D. Sun, J. S. Baker, Y. Gu, Running speed does not influence the asymmetry of kinematic variables of the lower limb joints in novice runners, *Acta of Bioengineering and Biomechanics*, Vol. 23, 2021, pp. 69–81  
<https://doi.org/10.37190/ABB-01742-2020-02>